

OPTICAL PROPERTIES OF DEFECTIVE SILICON CARBIDE NANOTUBES: THEORETICAL STUDY

PROPIEDADES ÓPTICAS DE NANOTUBOS DE CARBURO DE SILICIO DEFECTUOSOS: ESTUDIO TEÓRICO

A. A. GHOZLAN AND J. A. TALLA[†]

Department of Physics, Al al-Bayt University, Al-Mafraq - 130040, Jordan; jtalla@aabu.edu.jo[†]

Recibido 19/3/2019; Aceptado 5/5/2019

The optical properties of silicon carbide nanotubes with different orientations of Stone Wales defects were investigated for polarized light, unpolarized light and light incident through polycrystalline media. Density functional theory were used to study the effect of different orientations of Stone Wales defects on the optical properties of chiral (8, 4) silicon carbide nanotube. We monitored the corresponding changes in dielectric function, optical conductivity, absorption, reflection spectra, refractive index, and loss function. We found that introducing different orientations of Stone Wales defects to silicon carbide structure modified yet improved the optical properties of the nanotubes.

Se investigaron las propiedades ópticas de nanotubos de carburo de silicio con diferentes orientaciones de defectos de Stone Wales para luz polarizada, no polarizada, y luz incidente a través de medios policristalinos. Se usó la teoría del funcional de densidad para estudiar el efecto de diferentes orientaciones de los defectos de Stone Wales sobre las propiedades ópticas del nanotubo quiral (8,4) de carburo de silicio. Monitoreamos los cambios correspondientes en la función dieléctrica, conductividad óptica, absorción, espectro de reflexión, índice de refracción y función de pérdidas. Encontramos que el introducir diferentes orientaciones de defectos de Stone Wales en la estructura modificada de carburo de silicio logró mejorar las propiedades ópticas de los nanotubos.

PACS: Silicon carbide nanotube (nanotubos de carburo de silicio), 42.50.Wk; optical properties (propiedades ópticas), 42.70.Qs; Stone Wales defects (defectos de Stone Wales), 42.70.-a; and density functional theory (teoría del funcional de densidad), 61.46.-w

I. INTRODUCTION

The successes in synthesizing carbon nanotubes prompted experimental and theoretical efforts on producing other types of nanostructured material [1–6]. For instance, silicon nanostructures, especially silicon carbide nanotubes have been theoretically predicted and experimentally produced [7, 8]. Currently, silicon carbide nanotubes are the focus of intense theoretical and experimental research [5, 8, 9]. For example, silicon carbide nanostructures have been recently produced by numerous experimental works. Furthermore, theoretical studies based on density functional theory are known to be more reliable method to predict the properties of nanostructure material [7, 10–14]. The interest in silicon carbide nanostructures emerges primarily from their extraordinary properties including; high reactivity of the internal/ external surface, chemical inertness, high thermal conductivity, thermal stability, and much more [15–18]. Furthermore, silicon carbide nanotubes are one of the hardest materials which suites applications designed for operations at high temperature and radiation environments [16, 19, 20]. This could be attributed to their semiconducting nature, radiation resistance and high thermal conductivity [16, 19]. Besides, the polar nature of silicon carbide nanotubes can intrinsically be excellent sensors for detecting some toxic gases, including; HCN, HCOH, CO, and NO [10, 21, 23]. Moreover, theoretical calculations proved an increase in the binding energy of H₂ around 20% with silicon carbide nanotube compared with pure carbon nanotubes [24, 25]. This increase in the binding energy could be attributed to the

partially hetero-polar binding nature of the Si–C bonds [24]. Therefore, silicon carbide nanotubes could be considered as the most suitable candidate for hydrogen storage [4, 26, 27]. Furthermore, previous theoretical calculations prove that silicon carbide nanotubes are stable structures, with the most stability predicted for silicon-carbon ratio 1:1 [8]. Moreover, these calculations prove that these silicon carbide nanotubes are always semiconducting in nature.

Unlike carbon nanotubes, the band gap energy of silicon carbide nanotubes is weakly dependent on the tube chirality with direct band gaps for zigzag tubes and indirect gaps for chiral and armchair nanotubes [28, 29]. Besides, compared to carbon nanotubes, silicon carbide nanotubes are polar materials which exhibit some unusual physical properties(11). For example, zigzag silicon carbide nanotubes become piezoelectric material and exhibits second order nonlinear optical response [10, 30].

Stone Wales defect is a typical defect in silicon carbide nanotubes [1, 6, 13, 31]. Wang's et al in their investigations indicates that Stone Wales defects in silicon carbide nanotubes can be created by irradiation technique [17]. However, not many studies conducted on chiral silicon carbide; this could be ascribed to the complexity in modeling the structure and the calculations accompany it [30].

To the best of our knowledge, there are no theoretical and experimental studies addressing the optical properties of chiral silicon carbide nanotubes with different orientations of Stone Wales defects. Furthermore, no first principal studies

of the dielectric response as well as other optical properties of silicon carbide nanotubes have been reported. This might be attributed to the heavy demand on computer resources. Therefore, predictions of the effect of introducing different orientations of Stone Wales defects on the optical properties of silicon carbide nanotubes are strongly desirable. Besides, studying the optical properties of silicon carbide nanotubes is important for electro optical applications. The main objective of this work is to study optical characteristics of silicon carbide nanotubes and silicon carbide nanotubes with Stone Wales defects by first-principles calculations. Whereas, tuning the optical properties of silicon carbide nanotube will open a wide range of applications including; solar energy, Anti-reflection coatings, self-cleaning systems, ultraviolet light-emitting diodes, photo-catalysis and flat panel displays [1, 13, 31].

II. COMPUTATIONAL METHOD

In this theoretical work, we aim to study the optical properties of silicon carbide nanotubes that contain different orientations of Stone Wales defects. To achieve our goal, we simulated different orientations of Stone Wales defects on a chiral (8, 4) silicon carbide nanotube. Stone Wales defects could be created when Si-C bond rotated by 90 deg [1], whereas, for chiral silicon carbide nanotubes, there are three possible Si-C bonds that more likely to be rotated by 90 deg, (Figure 1). Consequently, three types with three different orientations of Stone Wales defects were created. The chiral angle (χ) were identified in such a way $0 \leq \chi \leq \pi/6$. Therefore, three different possible angles were identified, i.e. $\pi/3 - \chi$, χ and $\pi/3 + \chi$, with 19.11deg. Therefore, the angles of Stone Wales defects are 19.11deg (Type I), 40.89deg (Type II) and 79.11deg (Type III), refer to Figure 1. The results obtained from silicon carbide nanotubes that contain the three types of Stone Wales defects were compared with the results obtained with pristine silicon carbide nanotubes. We set the lattice constant "a" and "b" for all simulated structures to be large enough to eliminate any possible interaction with the tube and its image. However, the third lattice direction "c" was set to be exactly the same as the nanotube length in order to keep the tube periodicity. Density functional theory was performed with the aid of CASTEP code, whereas, all simulated structures were relaxed using geometry optimization calculations. Eigen functions were also calculated using self-consistent Kohn Sham equation. Furthermore, the revised Perdew Burke Ernzerhof (RPBE) sub-functional was used with generalized gradient approximation. While, the norm-conserving pseudo-potential was employed in reciprocal space, and an extended electronic wave functions into plane wave basis set with finite basis set correction were used. A 600 eV cutoff energy was assigned for the grid integration $1 \times 1 \times 18$ kpoints from Monkhorst-Pack scheme. To improve the calculation's accuracy, energy convergence tolerance was set to 5×10^{-5} eV. Moreover, we set the maximum force convergence tolerance and the maximum displacement was set to 0.01 eV/Å and 0.002 Å, respectively. To reduce the computational time,

we implemented DFT Semi-core Pseudopotential core treatment. We performed our optical calculations on chiral(8, 4) silicon carbide nanotube with three different orientations of Stone Wales defects. Finally, energy calculations were performed for all geometry optimized structures. We monitored the corresponding changes in dielectric function, optical conductivity, absorption, reflection spectra, refractive index, and loss function. We analyzed the obtained results to figure out the effect of introducing different orientations of Stone Wales defects on the optical properties of silicon carbide nanotubes [6, 31].

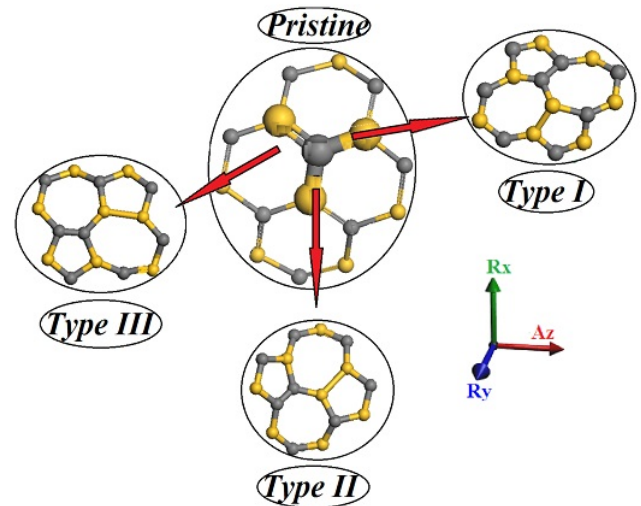


Figure 1. Schematic diagram represents different types of Stone Wales defects as well as the bonds that create the three types of Stone Wales defects.

III. RESULTS AND DISCUSSION

We studied the optical properties of silicon carbide nanotubes with different orientations of Stone Wales defects. To study all possible cases, three types of incident lights were used i.e. polarized and unpolarized light, as well as light incident through polycrystalline media. Three different orientations of Stone Wales defects were simulated on the surface of chiral (8, 4) silicon carbide nanotubes. To have a complete insight, six optical properties were extensively studied: dielectric function, optical conductivity, absorption, reflection spectra, refractive index, and loss function.

III.1. Dielectric function

Dielectric function ($\epsilon(\omega)$) could be used to characterize not only the optical properties of materials but also the materials electrical properties. Dielectric function can be calculated with the aid of the following equation:

$$\epsilon(\omega) = \epsilon_1(\omega) + \epsilon_2(\omega) \quad (1)$$

Where $\epsilon_1(\omega)$ is the dielectric function real part and $\epsilon_2(\omega)$ is the dielectric function imaginary part [13, 31].

III.2. Dielectric function real part

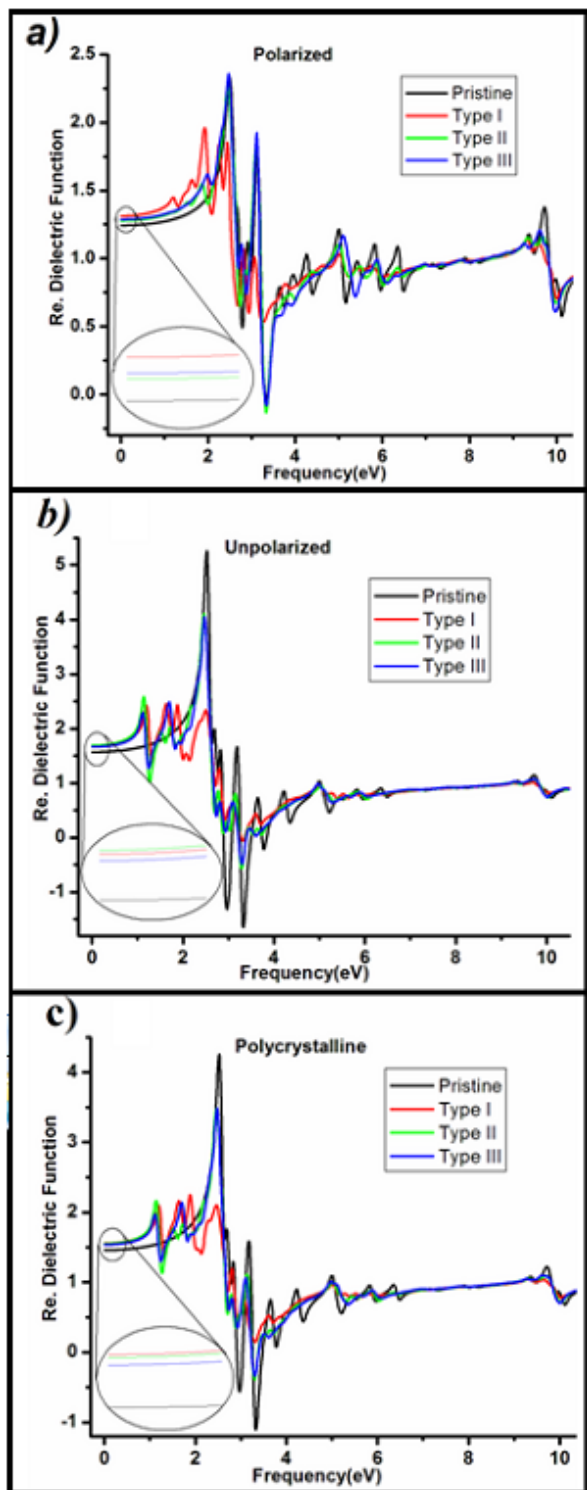


Figure 2. Real part of dielectric function for the three types of Stone Wales defects upon applying polarized light, unpolarized light and light incident through polycrystalline media.

We theoretically investigated the effect of different directions of Stone Wales defects on the dielectric function for silicon carbide nanotubes, by applying three different cases of incident light: polarized and unpolarized as well as light incident through polycrystalline media. The discrepancy in the dielectric function for all silicon carbide nanotubes

under investigation is a good indication that these silicon carbide nanotubes are anisotropic in nature (Figure 2 (a, b, c)). Whereas, the most obvious anisotropy occurs for unpolarized incident light and incident light through polycrystalline media cases, refer to Figure 2 (a, b, c). The maximum peak observed around 3-3.5 eV. Whereas, the most declared peak for pristine silicon carbide nanotubes observed when the incident light is unpolarized and the incident light through polycrystalline media. However these peaks are not clearly distinguished from each other upon applying polarized light. Furthermore, introducing different orientations of Stone Wales defects has direct impact on the dielectric function static value, whereas, this clear discrepancy in the dielectric function static value could attributed to the type of defects created by Stone Wales defects, refer to inset in Figure 2 (a, b, c). Moreover, some intermediate peaks observed at low frequency region. Whereas, this peak intensity decrease/increase depending on the incident light nature, refer to Figure 2 (a, b, c).

The dielectric function peaks originated from electron transitions between carbon $2p$ states and silicon $3p$ states in the π^* bond of silicon carbide nanotube. However, in higher energy range, no clear dielectric peaks were found. Compared with dielectric functions for the pristine silicon carbide nanotube, the mainly dielectric peak for different orientations of Stone Wales defects is suppressed, which has a direct relationship with the depression in the density peaks at high frequency range (Figure 2 (a, b, c)).

III.3. Dielectric function imaginary part

Although the dielectric functions real part oscillates between negative and positive values (Figure 3 (a, b, c)), the dielectric function imaginary part is positive throughout the whole range of frequency, refer to Figure 3 (a, b, c). Besides, the dielectric function imaginary part static value for all silicon carbide nanotubes under study is also positive which consistent with the continuous media theory. Furthermore, the imaginary part static value of dielectric function is always zero regardless the incident light nature and the type of Stone Wales defects, refer to Figure 2 (a, b, c). For polarized incident light, the maximum peak occurs for type III Stone Wales defects followed by type II. This peak originated around 3.25 (1/fs) and red shifts upon applying unpolarized incident light and light incident through polycrystalline media. Furthermore, upon applying unpolarized light and the incident light through polycrystalline media, the maximum values of the dielectric function imaginary part for all silicon carbide nanotubes under study occur around 2.75 (1/fs) at 4.5 eV and 3.75 eV, 1.75 eV, and 3.5 eV for pristine silicon carbide nanotubes and silicon carbide nanotubes with type I and type II and type III Stone Wales defects, respectively (Figure 3 (a, b, c)). Dielectric function peaks ϵ_2 can be divided into three parts; first part of dielectric peaks located at low frequency range. These peaks originated from transitions in the π^* bond. Second part of dielectric peaks originated from electron transitions from π bond to π^* bond which play a crucial role in the formation of dielectric peaks. The third part

of dielectric peaks located at higher frequency range. These peaks mainly originated from the electronic transitions from σ bond to σ^* bond.

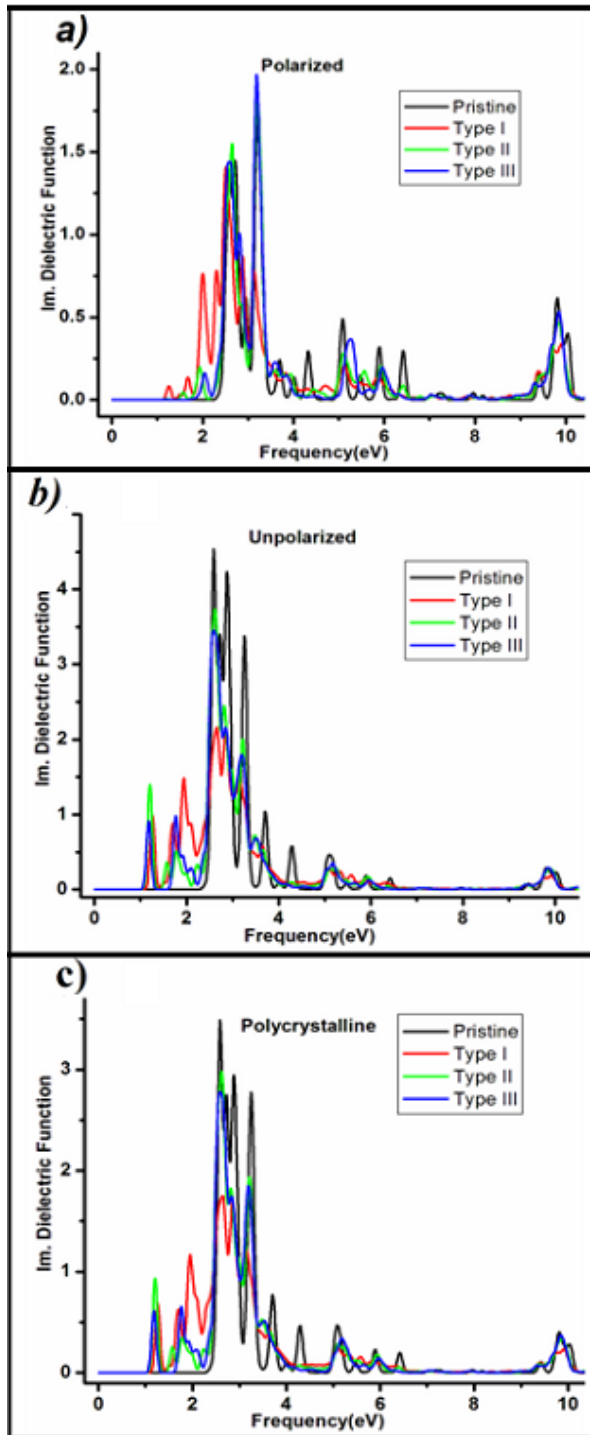


Figure 3. Imaginary part of dielectric function for the three types of Stone Wales defects upon applying polarized light, unpolarized light and light incident through polycrystalline media.

From the above, at different incident light nature, introducing different orientations of Stone Wales defects to pristine silicon carbide nanotube significantly modify the peaks intensity of the dielectric functions imaginary part.

III.4. Optical conductivity

Optical conductivity is defined when a material becomes more conductive as a result of absorption of electromagnetic waves. Figure 3 (a, b, c) represent the optical conductivity ($\sigma(\omega)$) for pristine silicon carbide nanotubes and silicon carbide nanotubes with Stone Wales defects at three different incident light nature i.e (polarized light, unpolarized light, and light incident through polycrystalline media). The optical conductivity ($\sigma(\omega)$) can be calculated using the following equation, whereas ϵ is the dielectric function,

$$\sigma(\omega) = i\omega 4\pi(1 - \epsilon) \quad (2)$$

Optical conductivity real part

Neither the type of the incident light nature nor the orientations of Stone Wales defects have any impact on the static value of the optical conductivity of silicon carbide nanotubes, refer to Figure 4 (a, b, c). This might be correlated to overlapping between valence and conduction bands at the Fermi level. Furthermore, it is clearly observed from Figure 4 (a, b, c) that the real part of the optical conductivity for all simulated silicon carbide nanotubes is strongest in the low frequency region, whereas, the maximum peak observed around 2.5-3.0 eV, with the highest peak related to pristine silicon carbide nanotubes for unpolarized incident light and light incident through polycrystalline media. In case of polarized incident light, the maximum peak observed in type III Stone Wales defects. Furthermore, in all cases of incident light, an intermediate peaks originated at lower frequency region, however, the optical conductivity of pristine silicon carbide nanotubes does not show up. For polarized incident light, the main peak of optical conductivity for pristine silicon carbide nanotube located around 3.25 eV with 0.7 (1/fs). However, upon applying unpolarized light, not only the main peak red shifts, but also a clear increase in optical conductivity value. Almost the same behavior observed upon introducing light incident through polycrystalline media with less increase in optical conductivity values compared to unpolarized case.

While type I Stone Wales defects behave differently, same behavior observed in other types of Stone Wales defects. For instance, in case of type I Stone Wales defects, blue shift observed in the main peak with slight increase in the optical conductivity values, refer to Figure 3 (a, b, c). From Figure 4 (a, b, c), it is clearly seen that, regardless the nature of the incident lights, the optical conductivity real part is positive. In addition, for polarized incident light, introducing type I Stone Wales defects to pristine silicon carbide nanotubes completely increase the optical conductivity real part, however, for unpolarized incident light and light incident through polycrystalline media, a clear decrease in the optical conductivity values. This could be attributed to the deformation occurs upon introducing Stone Wales defects. While introducing different orientations of Stone Wales defects create defects in the nanotube surface, a clear deformation observed in case of type I Stone Wales

defects.

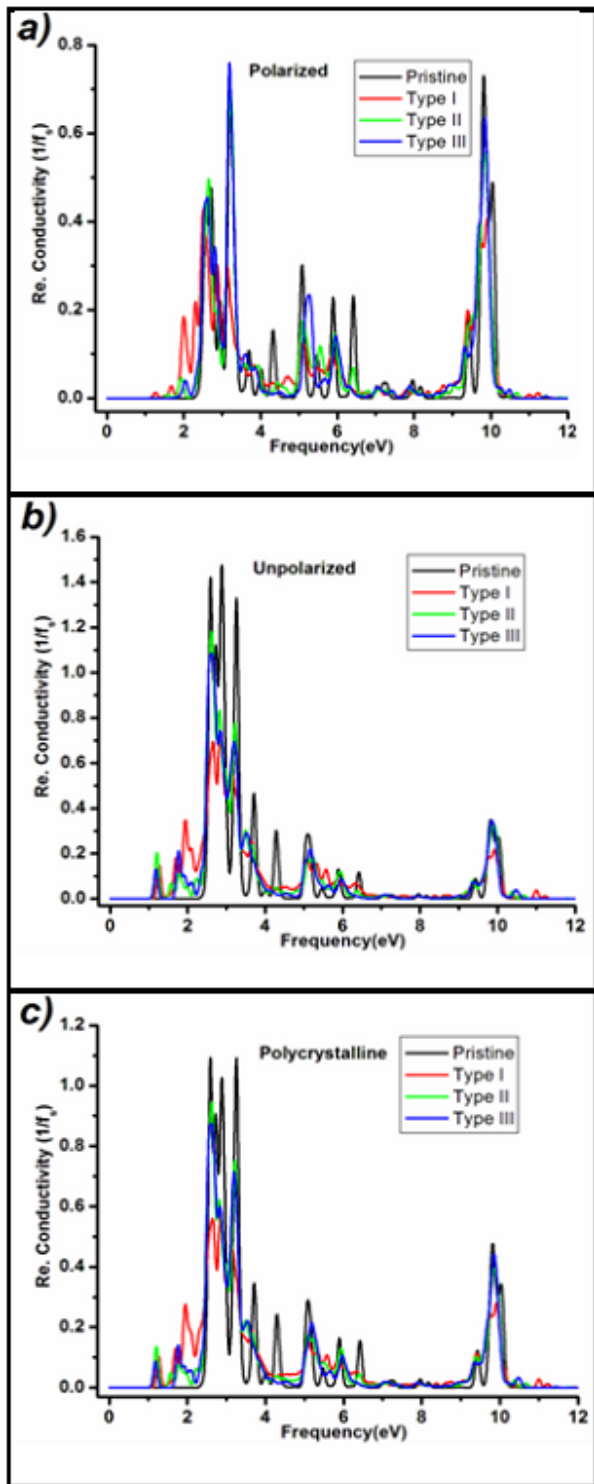


Figure 4. Real part of optical conductivity for the three types of Stone Wales defects upon applying polarized light, unpolarized light and light incident through polycrystalline media.

Optical conductivity imaginary part

The optical conductivity imaginary part has the highest peak intensity for type II Stone Wales defects nanotubes followed by type III Stone Wales defects when light is polarized. The minimum peak observed for type I of Stone Wales defects when light is polarized. In other words, when incident light is polarized, introducing type II and type III of Stone

Wales defects to pristine silicon carbide nanotube increase the optical conductivity imaginary part peak intensity.

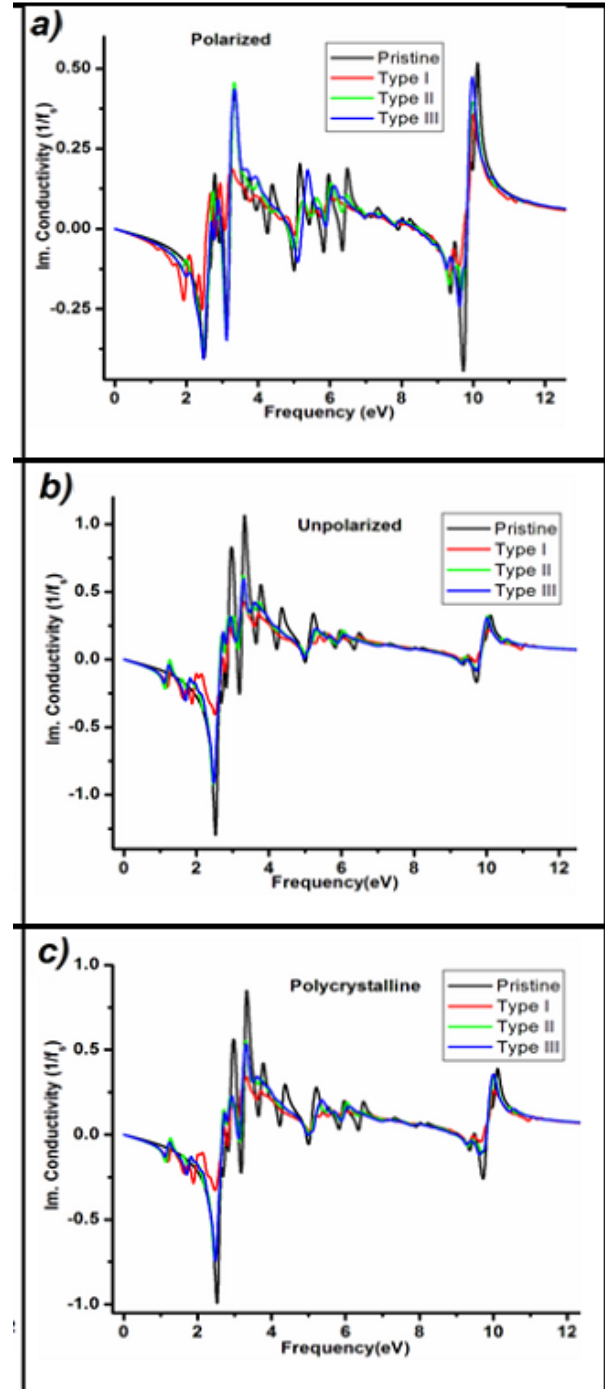


Figure 5. Imaginary part of optical conductivity for the three types of Stone Wales defects upon applying polarized light, unpolarized light and light incident through polycrystalline media.

For the same incident light, introducing type I Stone Wales defects to pristine silicon carbide nanotubes decrease the optical conductivity imaginary part peak intensity, refer to Figure 5 (a, b, c). This discrepancy in the three types could be attributed the orientation of Stone Wales defects and also to the amount of deformation occurred upon introducing Stone Wales defects, refer to Figure 5 (a, b, c). In case of unpolarized incident light and light incident through polycrystalline

media, pristine silicon carbide nanotube has the maximum values of optical conductivity imaginary part compared to other three types of Stone Wales defect. Besides, a clear increase in the pristine nanotube peak intensity compared to polarized incident light. For instance, the peak intensity for pristine silicon carbide nanotubes for polarized incident light is around 0.50 (1/fs). Upon applying unpolarized incident light and light incident through polycrystalline media, the peak intensity increased to 1.00 (1/fs) and 0.85 (1/fs) respectively. Moreover, some intermediate peaks appear at low frequency region like in case of polarized incident light. These peaks start to distinguish from each other when the incident light is unpolarized and incident light through polycrystalline media (5 (a, b, c)).

III.5. Absorption

Figure 6 (a, b, c) represents the absorption spectra for pristine silicon carbide nanotubes and silicon carbide nanotubes with Stone Wales defects for different incident light nature. The absorption spectra show anisotropy behavior in the optical properties in all silicon carbide nanotubes under study. For example, when the incident light is polarized, the strongest absorption peak located around the frequency 3.25 eV. These maximum peaks belong to type II and type III Stone Wales defects. The absorption peak significantly decreases upon introducing Stone Wales defects, refer to Figure 6 (a, b, c). Besides, the strong absorption peak appears in an ultraviolet region. Upon introducing different orientations of Stone Wales defects, and for the case of polarized light, the absorption peak was significantly increased. This could be ascribed to intrinsic indirect inter-band transitions along the band gap. Furthermore, regardless the incident light nature and in all silicon carbide nanotubes under study, the highest absorption peak occurs in the frequency range of about 3.0 - 3.5 eV. However, upon applying unpolarized and polycrystalline incident light, the behavior is quite different as the maximum absorption spectra observed for pristine silicon carbide nanotube. However, introducing different orientations of Stone Wales defects to the nanotube surface will significantly decrease the absorption spectra. Furthermore, for all incident light nature, type I of Stone Wales defect has the minimum absorption spectra. This could be directly correlated to the orientation of Stone Wales defects. The heptagon and pentagon rings created in the nanotube surface create special kind of deformation with protrude and intrude in the structure, this protrude and intrude significantly depends on the orientation of the heptagon and pentagon rings. Moreover, at low frequency region, no absorption spectra were observed for pristine silicon carbide nanotubes. However, for the same low frequency region, absorption starts to show up as a result of introducing different types of Stone Wales defects. This could be attributed to defects created at the surface of silicon carbide nanotubes, refer to Figure 6 (a, b, c). For all silicon carbide nanotubes, the absorption spectra display a significant anisotropy in wide range of ultraviolet region. Besides, the observed peaks in the absorption spectra is a

good indication that maximum absorption occurs at that specific energy; however, introducing different orientation of Stone Wales defect to silicon carbide nanotube surface significantly modify the absorption peak.

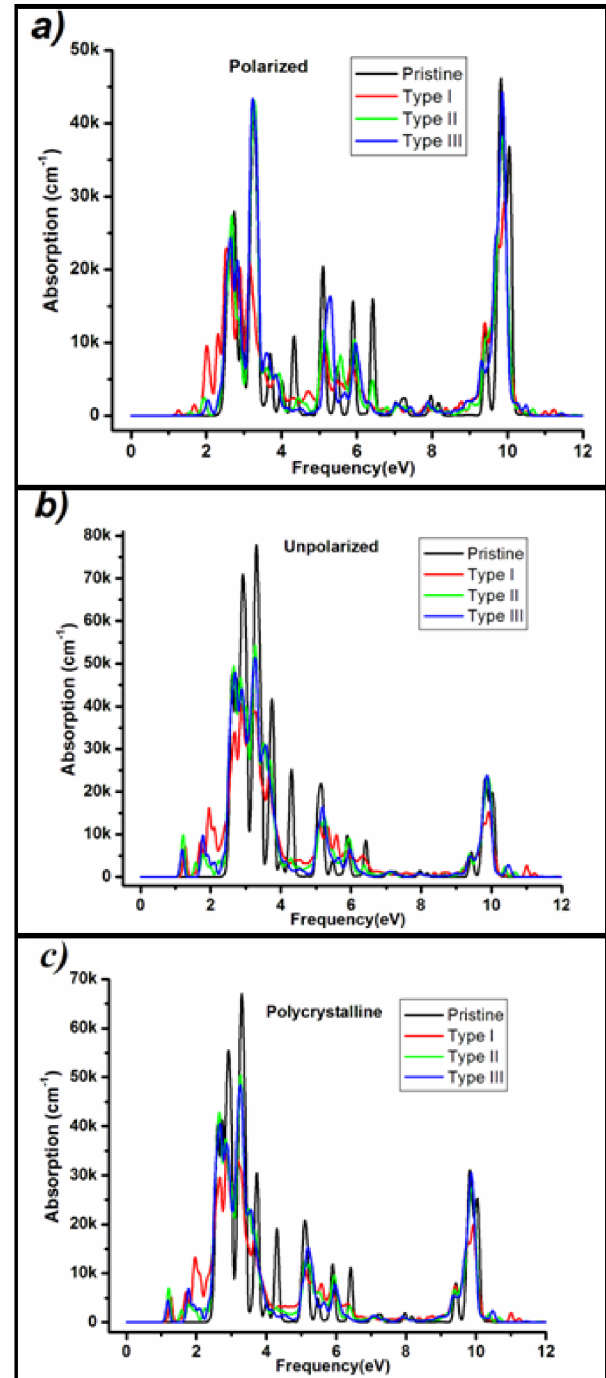


Figure 6. Absorption spectra for the three types of Stone Wales defects upon the applying: a) polarized light, b) unpolarized light and c) light incident through polycrystalline media.

The modification in the peak frequency and peak intensity could be attributed to semiconducting-metal phase transition as previously reported. Naturally, incident light peaks energies occur around 3.25 eV which attributed to inter π band transitions. Whereas, depending on the incident light nature, some peaks emerge while other peaks disappear,

refer to Figure 6 (a, b, c). For instance, in pristine silicon carbide nanotube when incident light is polarized a clear peak located around 3.0 eV. This peak completely disappear when the incident light is unpolarized and incident light through polycrystalline media. After all, and regardless the incident light nature, introducing different orientations of Stone Wales defects have a direct impact on the absorption spectra.

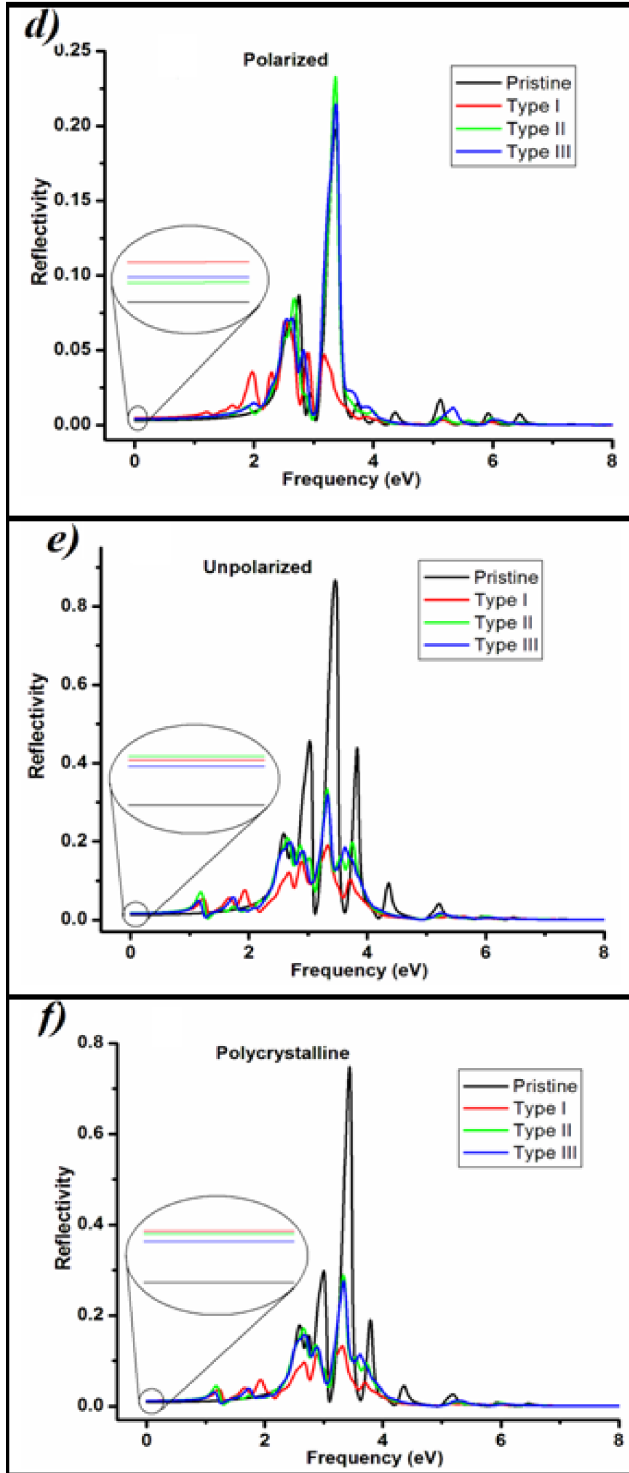


Figure 7. Reflectivity spectra for the three types of Stone Wales defects upon the applying: a) polarized light, b) unpolarized light and c) light incident through polycrystalline media.

III.6. Reflection spectra

Anti-reflection coatings were not only used for self-cleaning systems but also used to damp the transparent substrates reflectivity. Figure 7 (a, b, c) represents the reflectivity spectra for pristine silicon carbide nanotubes and silicon carbide nanotubes with different orientations of Stone Wales defects. Regardless the incident light nature, introducing different orientations of Stone Wales defects to pristine silicon carbide nanotubes structure have a significant impact to the reflectivity static value, refer to Figure 7 (a, b, c). For unpolarized light and incident light through polycrystalline media, introducing different orientations of Stone Wales defects significantly decreases the reflectivity main peaks. However, when light is polarized, the reflectivity main peak increases upon introducing different orientations of Stone Wales defects. Regardless the incident light natures, the main reflectivity peaks for all silicon carbide nanotubes under study occur around 3.25 eV, refer to Figure 7 (a, b, c). Besides, for all incident light nature, the reflectivity spectra are red shifted upon introducing Stone Wales defects to pristine silicon carbide nanotubes (Figure 7 (a, b, c)). Unlike pristine, type I, type II, and type III behaves differently when light is polarized as the reflectivity is significantly increased.

Furthermore, the static reflectivity value for pristine silicon carbide nanotubes significantly increased upon introducing Stone Wales defects to silicon carbide surface. The above behavior could be ascribed to anisotropy in reflection which becomes more declared upon introducing different orientations of Stone Wales defects.

III.7. Refractive-index

The refractive index can be calculated using the following equation:

$$n(x) = \sqrt{\frac{(\varepsilon_1^2 + \varepsilon_2^2)^{1/2} + \varepsilon_1^2}{2}} \quad (3)$$

Whereas, Figure 8 (a, b, c) represents the optical refractive indices for pristine silicon carbide nanotubes and silicon carbide nanotubes with different orientations of Stone Wales defects when light is polarized, unpolarized and light incident through the polycrystalline media. Clearly from Figure 8 (a, b, c) and regardless the incident light nature, the static refractive indices significantly increased upon introducing different orientations of Stone Wales defects to the nanotubes structure. The most pronounced increase occurs upon introducing type I to pristine silicon carbide nanotube. This increase in the static refractive index is a good indication that introducing different orientations of Stone Wales defects to pristine silicon carbide nanotubes has a direct impact in improving the optical properties anisotropy. Besides, for all incident light nature, introducing different orientations of Stone Wales defects to the nanotubes surface red shifts the refractive indices spectra, refer to Figure 8 (a, b, c).

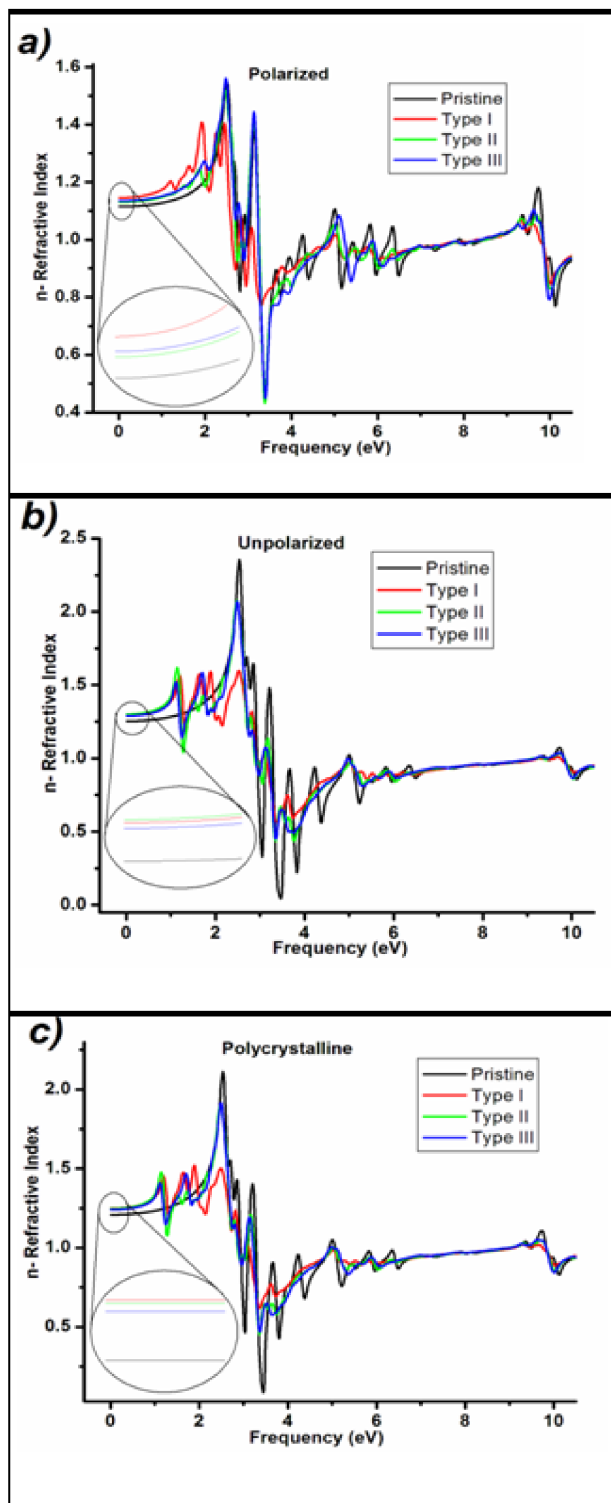


Figure 8. Refractive index for the three types of Stone Wales defects upon applying: a) polarized light, b) unpolarized light and c) light incident through polycrystalline media.

III.8. Loss function spectra

The loss function peak position represents the typical energy of the Plasmon's in the nanotubes under study. It can be calculated using the following equation:

$$Im = \left[\frac{1}{\varepsilon(q, \omega)} \right]. \quad (4)$$

The loss function spectra for pristine silicon carbide nanotube and silicon carbide nanotube with different orientations of Stone Wales defects were illustrated for polarized incident light, unpolarized incident light and light incident through polycrystalline media, refer to Figure 9 (a, b, c).

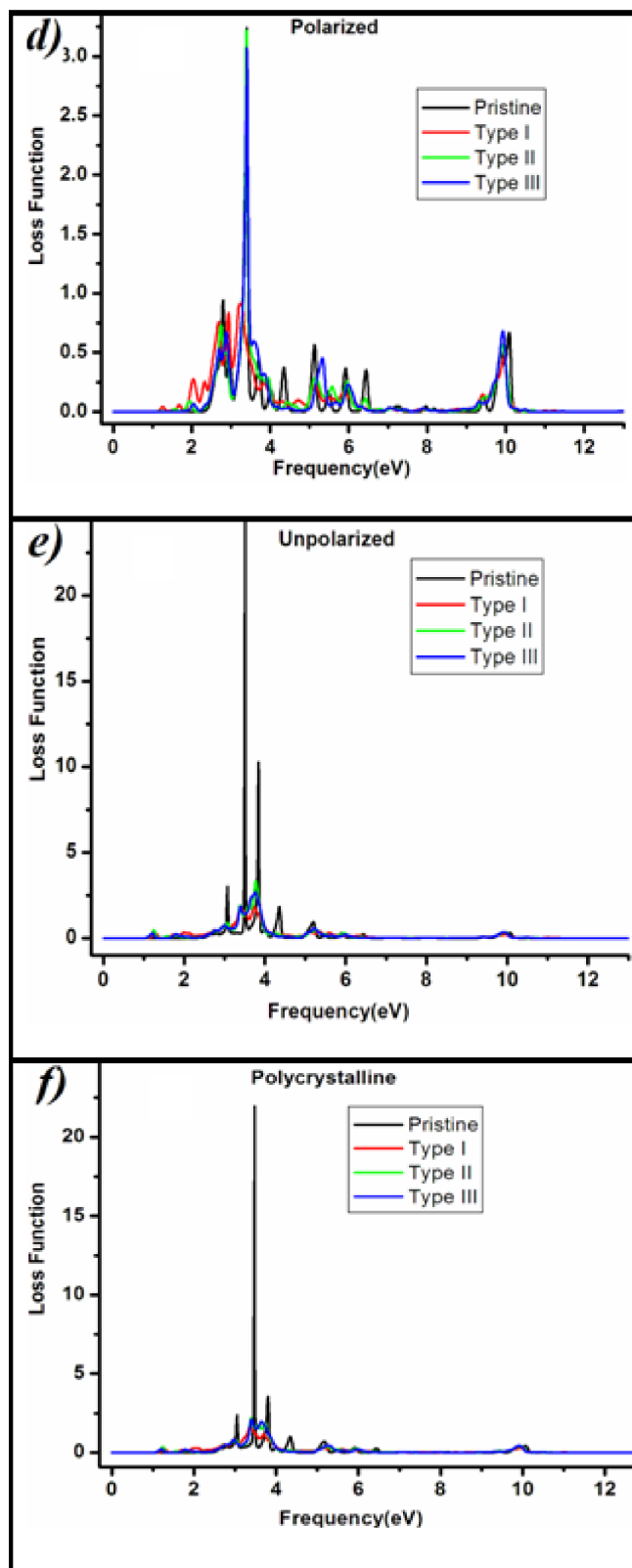


Figure 9. Loss function for the three types of Stone Wales defects upon applying: a) polarized light, b) unpolarized light and c) light incident through polycrystalline media.

When polarized light is used, the loss function magnitude for pristine silicon carbide nanotube is significantly decreased upon introducing three types of Stone Wales defects. This significant reduction in the loss function magnitude might be attributed to decrease in free charge carriers. In addition, the loss function spectra red shifted upon introducing different orientation of Stone Wales defects, refer to Figure 9 (a, b, c). This could be attributed not only to decrease in the Fermi energy but also to decrease in the total number of electrons.

IV. CONCLUSIONS

The optical properties of pristine silicon carbide nanotube and silicon carbide nanotube with different orientations of Stone Wales defects were studied for polarized and unpolarized light as well as light incident through polycrystalline media. With the aid of density functional theory, different optical properties were investigated, including; dielectric function, optical conductivity, absorption, reflection spectra, refractive index, and loss function. We have noticed that introducing Stone Wales defects plays a crucial rule on tuning the optical properties of silicon carbide nanotubes. Besides, introducing different orientations of Stone Wales defects to pristine silicon carbide nanotubes has a direct impact on dielectric function frequency. Therefore, depending on the nature of incident light, the peak intensity of the dielectric spectra real part has shown a clear decrease/increase upon introducing different orientations of Stone Wales defects. The discrepancy in the dielectric function for all silicon carbide nanotubes under investigation is a good indication that these silicon carbide nanotubes are anisotropic in nature. Furthermore, introducing different orientations of Stone Wales defects has direct impact on the dielectric function static value, whereas, this clear discrepancy in the static dielectric function value could attributed to the type of defects created by Stone Wales defects. Whereas, the most obvious anisotropy occurs for unpolarized incident light and incident light through polycrystalline media cases. In addition, and regardless the nature of the incident lights, the optical conductivity real part is all the way positive. Besides, for polarized incident light, introducing type I Stone Wales defects to pristine silicon carbide nanotubes completely increases the optical conductivity real part. However, for unpolarized incident light and light incident through polycrystalline media, a clear decrease in the optical conductivity values. For all silicon carbide nanotubes, the absorption spectra display a significant anisotropy in wide range of ultraviolet region.

Furthermore, introducing different orientations of Stone Wales defects to pristine silicon carbide nanotubes have a significant impact on the reflectivity static value. Moreover, the static reflectivity value for pristine silicon carbide nanotubes significantly increased upon introducing different orientations of Stone Wales defects to silicon carbide surface. Regardless the incident light nature, the static refractive indices significantly increased upon introducing different orientations of Stone Wales defects to the nanotubes structure. This increase in the static refractive index is a

good indication that introducing different orientations of Stone Wales defects to pristine silicon carbide nanotubes has a direct impact in improving the optical properties anisotropy. Finally, the loss function magnitude for pristine silicon carbide nanotube is significantly decreased upon introducing Stone Wales defects. In addition, the loss function spectra red shifted upon introducing different orientation of Stone Wales defects.

REFERENCES

- [1] J.A. Talla, *Advanced Science, Engineering and Medicine* **19**, e00378 (2019)..
- [2] B. Xu, J. Ouyang, Y. Xu, M.S. Wu, G. Liu, and C.Y. Ouyang, *Comput. Mater. Sci.* **68**, 367 (2013).
- [3] A. Wu, Q. Song, L. Yang, and Q. Hao, *Comput. Theor. Chem.* **977**, 92(2011).
- [4] J. Zhou, M. Zhou, Z. Chen, Z. Zhang, C. Chen, R. Li, X. Gao, and E. Xie, *Surf. Coat. Technol.* **203**, 3219 (2009).
- [5] *Phys. Lett. A* **383**, 2076 (2019).
- [6] J.A. Talla, *Computational Condensed Matter* **15**, 25 (2018).
- [7] H. Dong, Z. Guo, K. Gilmore, C. Du, T. Hou, S.T. Lee and Y. Li, *Nanotechnology* **26**, 275201 (2015).
- [8] R.J. Baierle, P. Piquini, L.P. Neves, and R.H. Miwa, *Phys. Rev. B* **74**, 155425 (2006).
- [9] J.A. Talla, *Computational Condensed Matter* **19**, e00378 (2019).
- [10] S. Behzad, R. Chegel, R. Moradian, and M. Shahrokhi, *Superlattices Microstruct.* **73**, 185 (2014).
- [11] J.A. Talla and A.F. Alsaliaby, *Chin. J. Phys.* **59**, 418 (2019).
- [12] J.A. Talla, K.A. Al-Khaza'leh, and A.A. Ghozlan, *Adv. Sci., Eng. Med.* **11**, 1 (2019).
- [13] J.A. Talla and A.A. Ghozlan, *J. Adv. Phys.* **7**, 33 (2018).
- [14] J. Talla, M. Abusini, K. Khazaeleh, R. Omari, M. Serhan, and H. El-Nasser, *Mater. Express* **7**, 516 (2017).
- [15] P. Partovi-Azar and A. Namiranian, *J. Phys.: Condens. Matter* **24**, 035301 (2012).
- [16] K. Adhikari and A.K. Ray, *Solid State Commun.* **151**, 430 (2011).
- [17] S.-J. Wang, C.-L. Zhang, and Z.-G. Wang, *Chin. Phys. Lett.* **27**, 106101 (2010).
- [18] K.M. Alam and A.K. Ray, *Phys. Rev. B* **77**, 035436 (2008).
- [19] Z. Wang, F. Gao, J. Li, X. Zu, and W.J. Weber, *J. Appl. Phys.* **106**, 084305 (2009).
- [20] H. El-Nasser and O. D. Ali, *Iran. Polym. J.* **19**, 57 (2010).
- [21] J.A. Talla, *Chem. Phys.* **392**, 71 (2012).
- [22] T. Jamal A, *Phys. B* **407**, 966 (2012).
- [23] A.A. Ahmad, A.M. Alsaad, B.A. Albiss, M.A. Al-Akhras, H.M. El-Nasser, and I.A. Qattan, *Phys. B* **470-471**, 21 (2015).
- [24] X. Wang and K.M. Liew, *The Journal of Physical Chemistry C* **116**, 26888(2012).
- [25] S. Karatas, H. El-Nasser, A. Al-Ghamdi, and F. Yakuphanolu, *Silicon* **10**, 651 (2018).
- [26] G. Alfieri and T. Kimoto, *Nanotechnology* **20**, 285703 (2009).
- [27] H. El-Nasser, *Appl. Phys. Res.* **9**, 5 (2017).

- [28] R.J. Baierle and R.H. Miwa, *Phys. Rev. B* **76**, 20 (2007).
[29] M. Yu, C.S. Jayanthi, and S.Y. Wu, *Phys. Rev. B* **82**, 075407 (2010).
[30] R. Ansari, M. Mirnezhad, and H. Rouhi, *Nano* **9**, 1450043 (2014).
[31] J.A. Talla, M. Nairat, K. Khazaeleh, A.A. Ghozlan, and S.A. Salman, *Computational Condensed Matter* **16**, e00311 (2018).

This work is licensed under the Creative Commons Attribution-NonCommercial 4.0 International (CC BY-NC 4.0, <http://creativecommons.org/licenses/by-nc/4.0>) license.

